RGD-Functionalized Superparamagnetic Nanoemulsions for Target-Specific Imaging of Tumor Angiogenesis

L. H. Deddens[1], P. A. Jarzyna[2], A. W. Griffioen[3], Z. A. Fayad[2], R. M. Dijkhuizen[1], and W. J. Mulder[2]
[1]Image Sciences Institute, University Medical Center Utrecht, Utrecht, Netherlands, [2]Imaging Science Laboratories, Mount Sinai School of Medicine, New York, United States, [3]Angiogenesis Laboratory Amsterdam, VU Medical Center, Amsterdam, Netherlands

Introduction

Nanoemulsions (NE) represent an attractive delivery platform for hydrophobic compounds since they improve their bioavailability and make their intravenous administration possible [1]. We have previously developed such a platform that consists of a hydrophobic core of soybean oil and iron oxide nanocrystals, and an amphiphilic corona of PEGylated lipids [2]. With MRI and near-infrared fluorescence (NIRF) imaging we demonstrated that NE passively accumulate in tumors. To expand their utility we report in this abstract their functionalization with $\alpha_v\beta_3$-specific RGD peptides to enable specific molecular MRI and optical imaging of tumor angiogenesis.

Methods

Superparamagnetic NE were composed of ordinary phospholipids, PEGylated lipids, maleimide functionalized PEGylated lipids, fluorescent lipids (rhodamine and Cy5.5), as well as soybean oil and superparamagnetic iron oxide nanocrystals (Fig. 1B). A lipid film was prepared from the aforementioned components, which was subsequently hydrated with a HEPES buffer and sonicated. Cyclic RGD peptides were conjugated via a sulfhydryl-maleimide coupling method. NE were characterized using dynamic light scattering and negative staining transmission electron microscopy (TEM).

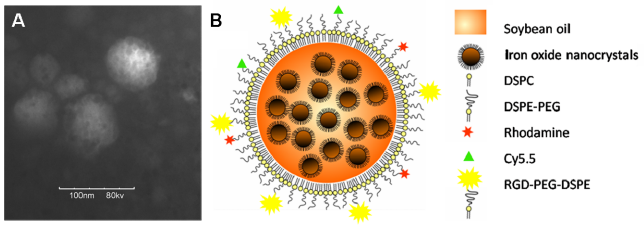

Figure 1. Negative staining TEM (A) and schematic representation (B) of RGD-NE.

Blood half-life and biodistribution of control NE and RGD-NE were conducted in mice (n = 3 for each group). Organs and blood samples were analyzed with quantitative NIRF imaging. Biodistribution was calculated from the NIRF signal of Cy5.5 originating from organs and was expressed as a percentage of total fluorescent signal after noise subtraction. Blood half-lives of NE were calculated from curves of decreasing Cy5.5 fluorescent intensities in blood samples over time.

In vivo MRI at 9.4 T of control NE and RGD-NE (n = 3 for each group) was conducted on mice bearing a subcutaneous LS147T tumor of a diameter around 1 cm. T_2^*-weighted images (FOV 2.56 cm x 2.56 cm, 128 x 128 matrix size, 10 slices of 1 mm, TE = 3 ms, TR = 120 ms, NT = 16) were acquired before and every 30 min for 3 h after intravenous injection of control or RGD-NE (15 mg/kg iron oxide nanocrystals). Isolectin-alexa488 (for vessel wall staining) was injected 10 min before sacrificing the animals, after which organs (liver, lung, spleen, kidney and tumor) were excised and snap-frozen. For confocal microscopy, tissue sections were fixed with DAPI-containing mounting medium. Perl's staining was applied to detect iron oxide in immunohistochemical sections.

Results and Discussion

Control NE and RGD-NE had a mean diameter of 90 ± 10 nm (Fig. 1A) and showed a similar blood half-life (control NE: 2.2 ± 0.6 h, RGD-NE: 1.6 ± 0.2 h) and biodistribution. 24 h after injection, highest NE concentration was found in clearance organs as liver (control NE: 53% ± 2%, RGD-NE: 53% ± 2%), spleen (control NE: 17% ± 0%, RGD-NE: 17% ± 4%) and kidney (control NE: 17% ± 1%, RGD-NE: 17% ± 1%).

Injection of control NE in tumor-bearing mice caused an initial decrease of signal intensity on T_2^*-weighted images in tumor tissue compared to pre-injection images (Fig. 2A), which restored during the next 3 h (Fig. 2B). This is reflective of passive perfusion of the control NE in tumor tissue. *Ex vivo* fluorescence imaging of tumor tissue showed low control NE fluorescence that was not co-localized with vessel wall staining (Fig. 2C). Perl's staining showed no iron present in the tissue (Fig. 2D). These data demonstrate that control NE did not bind specifically to tumor vessels.

MR images after injection of RGD-NE showed a lowering of signal intensity in the tumor periphery where angiogenesis activity is highest. This decrease was retained after 3 h (Fig. 2F) when compared to pre-injection images (Fig. 2E), which suggests specific binding. RGD-NE fluorescence co-localized with endothelial cell staining, as observed in tumor sections (Fig. 2G). Iron staining (Fig. 2H) further corroborated the presence of RGD-NE in tumor tissues.

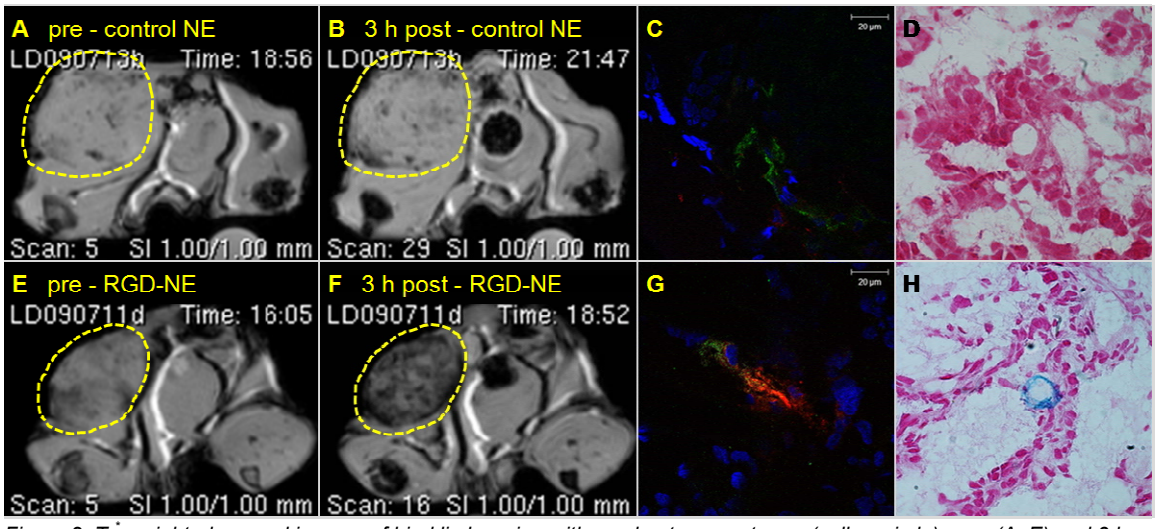

Figure 2. T_2^*-weighted coronal images of hind limb region with a subcutaneous tumor (yellow circle); pre- (A, E) and 3 h post-contrast injection (B, F). Fluorescence images (C, G) and Perl's staining (D, H) of tumor tissue. Injected contrast agent: control NE (A-D) or RGD-NE (E-H).

Conclusion

This study demonstrates that the nanoemulsion platform, developed for passive delivery of hydrophobic compounds to tumor tissue, is also very suitable for targeted applications. In the current study we applied $\alpha_v\beta_3$-targeted RGD-NE for molecular MRI of tumor angiogenesis and revealed a high degree of specificity by means of fluorescence microscopy and immunohistochemistry.

References

1. Sarker, D.K., *Engineering of nanoemulsions for drug delivery.* Curr Drug Deliv, 2005. **2**(4): p. 297-310.
2. Jarzyna, P.A., et al., *Iron oxide core oil-in-water emulsions as a multifunctional nanoparticle platform for tumor targeting and imaging.* Biomaterials, 2009. **30**(36): p. 6947-6954.